Columbia International Publishing
American Journal of Agricultural Science and Technology
(2013) 2: 45-60
doi:10.7726/ajast.2013.1004
Research Article

A Multispectral Sorting Device for Wheat Kernels

Tom Pearson*, Elizabeth Maghirang, and Floyd Dowell

Received 17 September 2012; Published online 16 March 2013

© The author(s) 2012. Published with open access at www.uscip.org

Abstract

A multispectral sorting device was constructed using three visible and three near-infrared light-emitting diodes (LED) with peak emission wavelengths of 470 nm (blue), 527 nm (green), 624 nm (red), 850 nm, 940 nm, and 1070 nm. The multispectral data were collected by rapidly (~12 kHz) blinking one LED at a time and subsequently measuring the reflected light from wheat kernels as they dropped off a feeder chute. A microcontroller was used to direct the LED pulses, digitize the analog signal from the photodiode, perform signal processing, and apply classifications. Sorting was accomplished through activation of an air valve that diverted the wheat kernels per the classification assignment. Three applications were tested; the separation of red from white wheat kernels, the separation of *Fusarium* head blight (FHB)-damaged kernels from undamaged kernels, and the separation of kernels classified as having high, medium, and low protein content. The performance of this LED-based sorter was compared with those of a high-speed color image-based sorter and a single-kernel near-infrared reflectance (SKNIR) sorter (950-1650 nm). The results indicate that the accuracy of the LED-based sorter was comparable to or better than the color image-based sorter. For the sorting of red from white wheat, the LED-based instrument removed 98% of the white wheat while also removing 23.7% of the red wheat in two subsequent passes. In contrast, the color image-based sorter removed less white wheat (83%) while removing more of the red wheat (42.4%). For FHB-damaged kernels, both the LED- and color image-based sorters removed approximately 90% of the kernels with visible symptoms of FHB-damage. However, the LED-based sorter removed fewer undamaged kernels (1.9%) compared to the color image-based sorter (7.0%). For isolating kernels with high protein content, both the LED and color image instruments diverted ~40% of the original wheat sample, which contained ~1.0% higher protein content on average than the original sample. However, the LED sorter was more consistent in isolating the higher-protein kernels across seven different varieties of hard red winter wheat. In comparison, the SKNIR sorter yielded a 1.9% increase in protein content compared with the original unsorted wheat sample. The throughput of the LED sorter was approximately 20 kernels/s compared with ~200 kernels/s for the image sorter and ~0.5 kernels/s for the SKNIR sorter. The cost of the LED-based sorter is expected to be less than either of the other two instruments; in total, the parts for the construction of the LED-based sorter cost approximately $1000. The LED-based sorter will likely be most effectively employed to separate the desired traits of small lots of seed (e.g., breeder size samples), assist in sample purification, and help breeders in selecting the kernels with higher protein and less damage due to FHB.

Keywords: Grain; Segregate; Optical

*Corresponding e-mail: thomas.pearson@ars.usda.gov
USDA-ARS-CGAHR, 1515 College Ave, Manhattan, KS, USA

Exhibit 1013

1. Introduction

Multispectral measurements taken with a limited number of spectral bands have been demonstrated as useful in the identification of certain kernel traits (Pasikatan and Dowell, 2004; Hansen et al., 2006; Delwiche, 2008; Shahin and Symons, 2009; Jaillais et al., 2012). Traditionally, the reflectance at the desired spectral bands was acquired using a filter wheel or tunable filter system. Although these systems are highly adaptable, they are inherently slow and can be costly. With the development of low-cost spectrometers, multispectral systems have been used primarily for certain imaging systems. Nevertheless, the small sensor element sizes of modern spectrometers require integration periods of at least several hundred milliseconds to acquire spectra with acceptable signal-to-noise ratios. Thus, these systems are not well-suited for sorting applications in which throughputs of at least 2 kg/hr (~20 kernels/s) of wheat require integration periods of less than 10 ms.

Light-emitting diodes (LEDs) are low-cost, and can be used for rapid multispectral measurements. In such a system, a series of LEDs that emit light in different spectral bands can be rapidly pulsed one at a time to quickly illuminate an object with light from several different spectral bands. The light reflected from an object can then be focused onto a single sensor. Because the sensor can be large enough to capture all of the focused light, the signal is 100 to 1000 times greater than can be produced from a single photodiode element of a spectrometer. This method has been used to sort almonds with defects (Pearson, 1999), to identify wheat kernels based on color and damage due to fungi (Delwiche, 2008), and to quantitatively measure chemical reagent colors (Yeh and Tseng, 2006). However, these instruments are relatively expensive to construct, and they are not directly adaptable to rapidly sorting kernels. The almond sorter (Pearson, 1999) used an analog multiplexing system to measure the transmittance of the almonds, an approach that required expensive circuitry and digital signal processing hardware. The instrument developed by Delwiche (2008) for inspecting wheat demonstrated the feasibility of such a system, but the device used only two LEDs (red and green). The accuracy of this system was also modest, and the system was based on the use of expensive prototyping electronics. The system developed by Yeh and Tseng (2006) represented a significant step forward in reducing the cost of LED multispectral instruments because their design employed a low-cost microcontroller, making the overall cost less than $20. However, their LEDs required manual switching, which, for all practical purposes, rendered this instrument unsuitable for high-speed inspection.

Automated sorters can aid wheat breeders to select desired grain traits or to remove seed impurities. Often, early-generation breeding populations consist of low-quantity seed samples that weigh less than 1000 g, but a breeder may have several hundred samples that must be sorted in a relatively short time period between harvest and planting. An SKNIR InGaAs-based spectrometer (Dowell et al., 2006) has been widely used for separating wheat by protein content, hardness, waxy characteristics, and objective FHB damage assessment. This spectrometer uses a spectral range of 950-1650 nm and can be highly accurate in selecting on the basis of these kernel characteristics. However, even though the kernel feeding and sorting of the SKNIR is automated, the throughput is only approximately 30 kernels/min. Thus, the use of the SKNIR can take approximately 16 h to sort a 1000 g sample. Wheat breeders have widely used a color image-based sorting device (Pearson, 2010) for separating kernels from populations, segregating for kernel color, removing FHB-damaged wheat, and removing weed seeds from samples. This instrument operates at a high speed

and can process ~200 wheat kernels/s (~300 g/min). The device is currently commercially available from the National Manufacturing Co., Lincoln, Nebraska at a cost of approximately $13000. However, this instrument is based only on visible light and has not been tested for its ability to separate wheat kernels by protein content. Automated sorters are becoming increasingly popular, and they enable crop breeders to respond to the demand for quality traits and grain industry end-users to respond to quality control issues. Furthermore, the automated sorters can contribute to hastening variety development by increasing the throughput of seed processing and selection and by possibly reducing some field rouging (manually removing) variant plant types. However, the cost of sorters remains prohibitive, and the mechanical feeding hardware of the currently available sorters, such as the 300 g/min image-based sorter (Pearson, 2010), may not be optimal for certain applications. There is a need for an affordable, general-purpose sorter that can separate kernels on both a visual and NIR basis and has a throughput of at least 1 kg/hr. The objective of this study was to assess the feasibility of using a low-cost LED-based multispectral sorting instrument to extend kernel-sorting capabilities beyond those enabled by an image-based sorter and to more rapidly perform sorting tasks similar to those enabled by the SKNIR

2. Materials and Methods

2.1 Description of the designed LED-based sorter

The LED-based sorter was designed to be low-cost, rapid, and able to measure light at six different spectral bands throughout the visible/NIR region. These performance specifications were met by pulsing the different LEDs at a rate of approximately 12 kHz such that a complete cycle through all six LEDs could be performed at a rate of approximately 2 kHz. The reflectance from the wheat kernels was measured as the kernels dropped off a 20 cm long feeder chute inclined at 45° above the horizontal. At this angle and chute length, the kernels travel at a speed of approximately 1.5 m/s. Thus, a series of six LED pulses are acquired in the time that a kernel travels a distance of approximately 0.75 mm. At this pulse rate, 15 cycles through the six different LEDs can be acquired while the kernel is in the sensor's field of view.

A microcontroller (ATmega328P Atmel Corp., San Jose, CA, USA) was used to control the timing of the LED pulses, digitize the analog signal from the photodiode, process the signal, perform the classifications, and activate an air valve which diverted the kernels according to the classification. The use of this microcontroller allows a throughput of approximately 20 kernels/s. An image of the printed circuit board with the LEDs, optics, and microcontroller is shown in Figure 1, and an electrical schematic of the device is shown in Figure 2.

The six different types of LEDs used in the construction were chosen to cover as broad a spectral range as possible. The peak emission wavelengths of these LEDs were: blue-470 nm (C503B-BAS-CY0C0462, Cree, Inc., Racine, WI, USA), green-527 nm (C503B-GAS-CB0F0792, Cree, Inc., Racine, WI, USA), red-624 nm (C503B-RAS-CY0B0AA, Cree, Inc., Racine, WI, USA), 850 nm (SIR-568ST3F, Rohm Semiconductor, San Diego, CA, USA), 940 nm (TSAL6100, Vishay Semiconductors, Shelton, CT, USA), and 1070 nm (L1070-03, Marubeni America Corporation, Santa Clara, CA, USA). All of the LEDs emit light as a narrow spot beam with a projection angle of approximately ± 15° from the LED axis. Additionally, the emission spectra of the LEDs approximated a Gaussian curve with a full width at half maximum (FWHM) of approximately 50 nm centered about the peak emission wavelength. A bank of three LEDs of each type (blue, green, red, 850 nm, 940 nm, and 1,070 nm)

was connected in series and arranged in a circular pattern (Figure. 1) around the lens to provide even illumination of the kernel. Each LED bank was switched with a bipolar NPN transistor (PZT2222A, Fairchild Semiconductor, San Jose, CA, USA) using a digital pulse provided by the microcontroller. Compared with the red and NIR LEDs, a higher supply voltage (15 V) was required for the blue and green LEDs. The higher voltage was maintained using two different voltage regulators to reduce and prevent excessive heat generation by the current limiting resistors for each bank of LEDs.

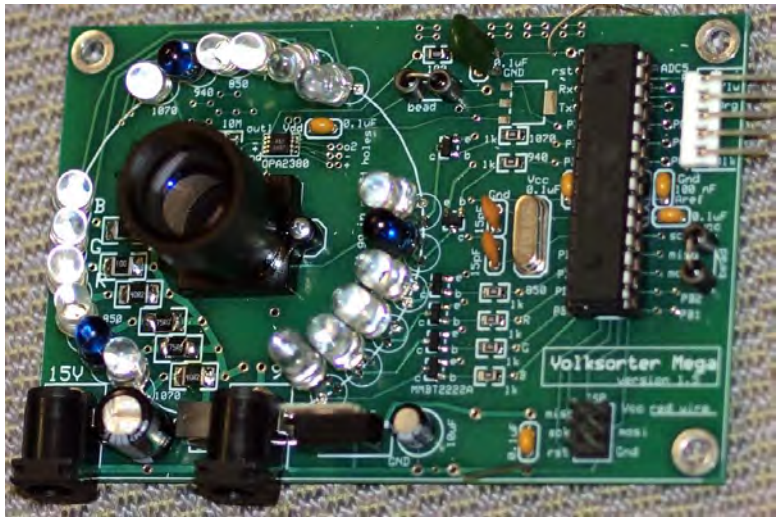

Fig 1. Circuit board with LEDs, microcontroller, transimpedance amplifier, and optics. Note that three sets of six LEDs provide even illumination about the kernel

The light reflected from the kernels was collected by a miniature lens with a 16 mm focal length (V-4316-2.0, Marshall Electronics, Inc., CA, USA), and was focused onto a photodiode (PDB-C171SM, Advanced Photonix, Inc., Ann Arbor, MI, USA). The photodiode was 2.77 mm x 2.77 mm, sufficiently large to accommodate all of the focused light from the lens thus maximizing the signal generated with the small amount of light reflected from the kernel. The output of the photodiode was amplified by a high-speed transimpedance amplifier (OPA2380AIDGKT, Texas Instruments, Dallas, TX, USA) connected in photovoltaic mode (Palais, 1988) to reduce the dark current noise. The amplified signal was routed through a passive low-pass RC filter (cutoff frequency = 160 kHz) to remove the higher-frequency noise before connecting to an analog-to-digital (A/D) port on the microcontroller.

Each bank of LEDs was pulsed "on" for 80 μs. Because the signal from the transimpedance amplifier would stabilize 30 μs after the LEDs were switched, the microcontroller was delayed for 30 μs after switching of the LEDs to initiate an A/D conversion. This microcontroller has the ability to perform conversions with 10-bit resolution; however, to decrease the time required for A/D conversions, only the highest 8 bits were used, a process that required 50 μs to perform. After a conversion was completed, the controller added the resultant conversion value to a running sum for each bank of LEDs, switched the current to another LED bank, and performed this process again. A total of 15 cycles for all LED banks was performed while a single kernel was in the field of view.

When no kernel was in the sensor's field of view, only the red LED was pulsed because the signal from the red LED was among the largest of the LEDs used. Data acquisition and switching to other LED banks was initiated by the microcontroller when the amplified photodiode signal rose to over 0.5 V, after which the microcontroller would proceed to pulse all of the LED banks sequentially for 15 cycles, integrate the photodiode signal from each LED bank, and return to a data analysis and classification procedure (as discussed below).

If the classification indicated that the kernel should be diverted, a digital pulse with a 10 μs duration was sent from the microcontroller to a timer circuit (Figure. 2). The timer circuit then sent a second pulse with a 8 ms duration to a solid-state relay (DO061B, Crydom Inc., San Diego, CA, USA) used to activate a solenoid air valve (36A–AAA–JDBA–1BA, Mac Valves, Inc., Wixom, MI, USA), which, once activated, diverted the kernels with a short blast of air. This scheme allowed the microcontroller and timer circuit to operate in parallel and allowed the microcontroller to collect the kernel information while the timer circuit controlled the air valve on an adjacent kernel. A schematic showing the configuration of the main sorter components is shown in Figure 3.

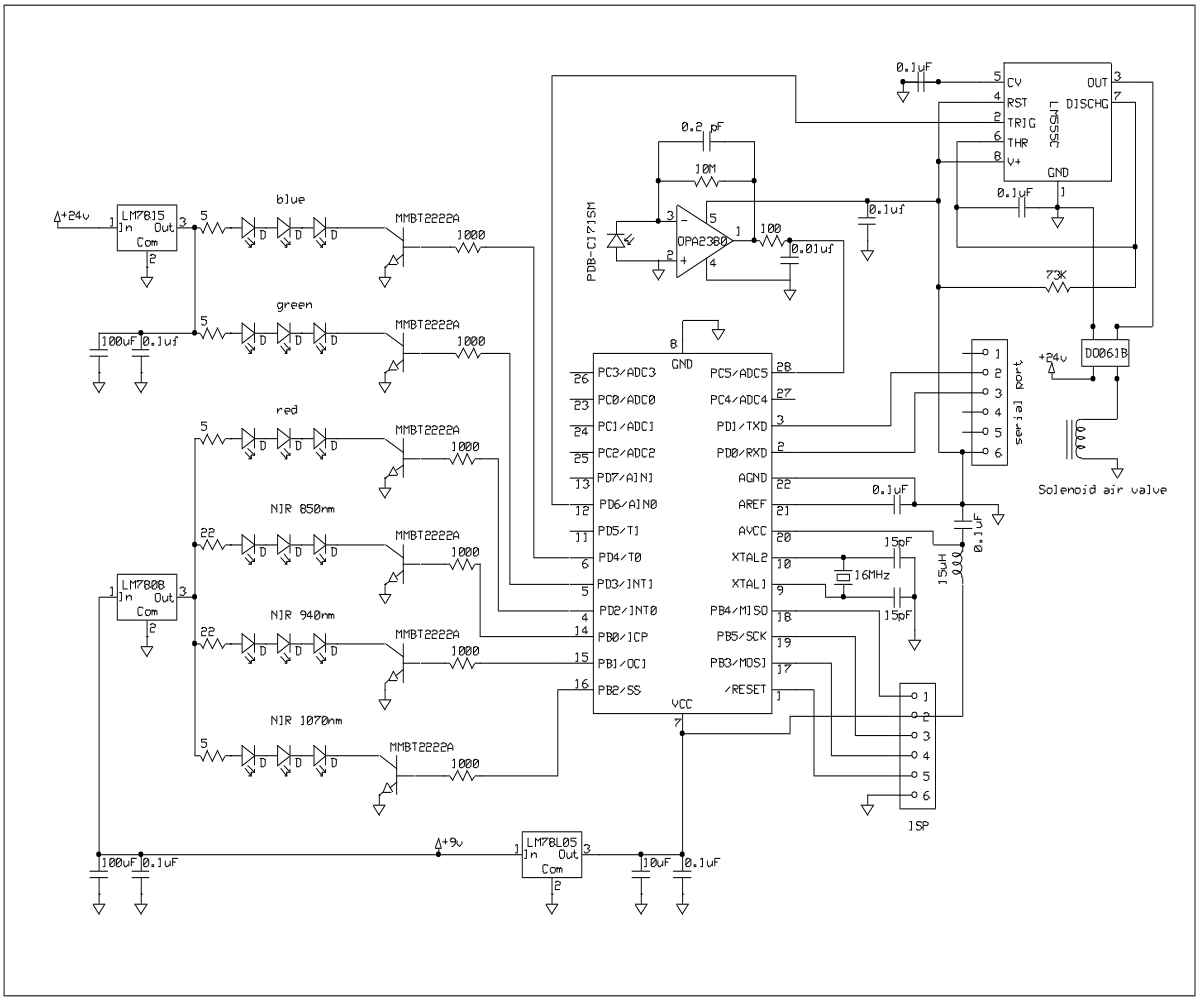

Fig 2. Schematic of the pulsed LED circuit

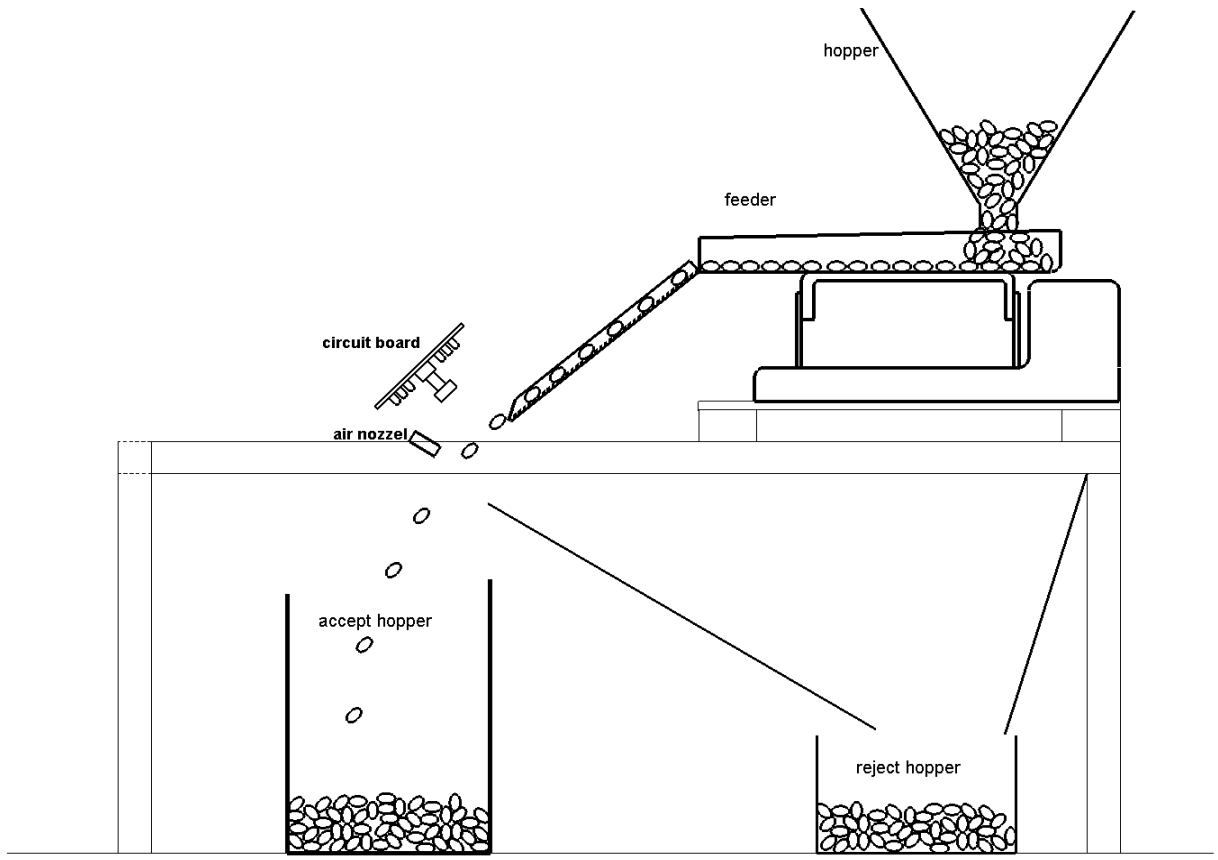

Fig 3. Schematic of the main sorter mechanical components

Operation of the sorter consisted of two modes; training and sorting. For the training mode, the photodiode outputs and potential discriminant features as described below were computed by the microcontroller and input to a PC, while samples of known classification were passed through the instrument. A discriminant function was computed based on the three most appropriate features. Once the discriminant function parameters were loaded onto the microcontroller, the PC was not required and the microcontroller captured photodiode outputs at the appropriate wavelengths, computed the required features and the discriminant function classified the kernels.

At start-up, when no kernels were being fed through the sorter, the microcontroller pulsed the six banks of LEDs 15 times to acquire a background light reading for each of the LED banks. These readings were subtracted from the integrated reflectance reading for each LED bank. For training mode, with a kernel in the field of view and after 15 pulse cycles were acquired from all six LED banks, the microcontroller performed calculations to produce a total of 22 features that could potentially be used for classification. Six of the features consisted of the integrated reflectance readings subtracted by the respective background readings. Three color chromaticity values were computed, as shown in Equation 1.

$$r = \frac{R}{R+G+B} \qquad (1)$$

where r is the chromaticity for the red LED, and R, G, and B are the integrated reflectances subtracted by the background readings for the red, green, and blue LEDs, respectively. The chromaticity values for the green and blue LEDs were computed in a similar manner. Three similar ratios were computed for the three NIR LEDs, as shown in Equation 2.

$$c_{850} = \frac{X}{X+Y+Z} \qquad (2)$$

where c_{850} is the fraction of the NIR LED at 850 nm compared to the sum of the other three NIR LED responses, and X, Y, and Z are the integrated reflectances subtracted by the background readings for the 850 nm, 940 nm, and 1070 nm LEDs, respectively. In addition, five ratios of the LED responses were computed: B/R, R/X, Y/X, Z/X, and Y/Z. Five differences between the LED responses were computed: R-B, X-R, X-Y, X-Z, and Y-Z.

The microcontroller was able to perform all required calculations in 100 μs, corresponding to the time required for the kernel to travel 0.15 mm, an insignificant distance for real-time sorting. As discussed below, the microcontroller used a three-feature discriminant function to perform the classifications. The feature selection and function parameters were computed on a personal computer (PC) with the data generated by the microcontroller and then transferred to the PC via a RS-232 protocol. Once the features and function parameters were loaded onto the microcontroller, the PC was not needed for sorting. Testing indicated that the instrument had a throughput of 15 to 25 kernels/s (1.6 to 2.7 kg/h), and the total materials used in its construction cost less than $1000 US.

2.2 Wheat Samples

Three sets of wheat samples were obtained for the test sorts. For sorting based on color, six hard wheat samples (Figure 4) were prepared by spiking each of the two hard red winter (HRW) wheat foundation seed samples (Jagger and Fuller) with 10% (by weight) of one of the three hard white wheat samples (Arlin, Klassic, and Madsen). For the FHB-damage sort, six HRW wheat samples (Art, Everest, Fuller, Overley, Santa Fe, and Tomahawk) with visual damage due to FHB were obtained from the 2010/2011 FHB wheat trials at Kansas State University (Manhattan, KS). Based on visual inspections of the 400 representative kernels, the level of FHB damage within the six samples ranged from approximately 10 to 30%.

Fig 4. Hard red winter (top) and hard white winter (bottom) wheat samples used in the sorting experiments.

For protein content sorting, seven HRW wheat samples were obtained from the 2011 harvest in Kansas. These samples included two from foundation seed sources (Jagger and Fuller) obtained from Kansas State University's Department of Agronomy (Manhattan, KS, USA) and five from commercial seed sources (Armour, Art, Everest, Santa Fe, and Winter Hawk) provided by Star Seed (Osborne, KS, USA). The commercial samples were cleaned by sieving out small, shrunken, and broken kernels using a 1.63 x 9.53 mm oblong sieve and by manually removing larger foreign material such as chaff and straw from the samples.

As needed, all samples were subjected to multiple passes through the Boerner divider (Seeburo Equipment Company, Des Plaines, IL, USA) to reduce the size of the samples to the quantities necessary for the various tests. This protocol also ensured that a representative subset of samples was maintained and used for all tests.

2.3 Instrumentation for Grain Sorting

The performance of the LED-based sorter was compared with two commercial instruments for sorts based on color (red versus white kernels), FHB damage (undamaged versus FHB-damaged kernels), and protein content (high-, medium- and low-protein kernels). The commercial instruments consisted of the Perten Single Kernel Near-Infrared Reflectance (SKNIR) Sorter (Stockholm, Sweden) and the High-Speed Color Image Sorter (National Manufacturing Co., Lincoln, NE, USA). Both instruments were previously developed at the USDA-ARS Engineering and Wind Erosion Research Unit, Manhattan, KS. All three instruments were used for protein sorting, whereas only the color image and LED sorters were used for the kernel color and visual FHB-damage sorting.

The SKNIR used for sorting based on the protein content automatically positioned individual wheat kernels in a viewing area, where an NIR spectrum was collected. The kernels were subsequently

sorted according to predefined quality cutoffs or criteria. The applied protein content calibration was developed using a partial least squares regression from 97 hard red winter wheat samples (Dowell et al., 2006). An initial protein content prediction for 200 kernels of each sample was obtained using the protein content calibration. The protein content distribution in each sample served as the basis for cutoffs selected to deliver 15% of the lowest protein content to Bin 1 and the highest 15% protein content to Bin 4, whereas Bins 2 and 3 contained 70% of the original sample and were expected to have kernels with an intermediate protein content. The sorting continued until each of Bins 1 and 2 contained at least 40 g of kernels.

The sorts using the color image and LED sorters were performed at their respective default reject thresholds, which was a 50% probability of one class or the other. The preliminary results indicated that this threshold level provided the best separation based on protein content. If the computed probability from the discriminant function for rejection was greater than or equal to 50%, the air valve was activated to reject the kernel. The red-white samples and FHB samples were sorted twice by both the color image and LED sorters. After the first sort, the samples classified as red for the red-white sort or as undamaged for the FHB sort were passed through the sorter a second time to remove additional white wheat or FHB-damaged wheat kernels that were missed during the first pass. Three sorting operations were used for the protein content sort. In this sort, the high protein content kernels were rejected, and the low protein content kernels were accepted. After the first pass through the sorter, the diverted kernels were sorted a second time, and the kernels that were rejected twice were called the "high" protein content lot. The kernels that were accepted during the first pass were also run through the sorter a second time, and kernels accepted twice were called the "low" protein content lot. Kernels that were rejected once and accepted once during these three sorting operations were blended and called the "intermediate" protein content lot.

2.4 Calibration of the color image and LED sorters

For both of the image- and LED-based sorters, the calibrations were accomplished using 200 kernels from each of the two contrasting classes to be segregated using a procedure developed by Pearson (2010). A two-way discriminant classifier was developed using the data from 200 kernels of each class. The kernels were fed through each instrument, and the image features produced by the color sorter or the 22 LED features previously discussed were transferred to a PC through their respective RS-232 ports. The PC used a discriminant analysis procedure to exhaustively search through the set of features extracted from the image or LED data and select three of these features to use for classification during sorting. The chosen features and discriminant function were then transferred back to the instruments to perform the sorting, and the reported classification accuracies are those from sorting samples with different kernels than were used for the calibrations.

For the red-white sorts, the LED and color image sorting devices were calibrated with a blend of Jagger and Fuller HRW varieties and a blend of Madsen, Arlin, and Klassic hard white varieties. For the FHB sorts, 200 kernels that exhibited a chalky white appearance distinctive of damage due to FHB were hand-picked from a commercial blend of HRW seed. Similarly, 200 undamaged or symptomless kernels were picked from the same sample and used as the sound sample for the calibration. For the protein content sort, 200 kernels from a commercial sample were hand-picked and assigned as "low protein" or "high protein" based on their visual appearance. The low-protein

set consisted of visually larger kernels that had a lighter or yellow appearance as these are noted for lower protein (Sharma et al., 1983), whereas the high-protein set consisted of visually darker and more vitreous kernels as these have been noted as having higher protein (Dexter et al., 1989).

2.5 Wheat Color Determination

After sorting, a NaOH test kit was used according to a procedure optimized by Ram et al. (2002) to enhance the kernel color differences and visually determine the true percentage of red and white wheat kernels in samples. For each sample, 100 kernels were manually subsampled and placed in a test tube, to which ~10 mL of a 20% NaOH solution was added. The tubes containing the solution and wheat kernels were placed in a preheated 60°C water bath for 10 min, after which the NaOH solution was drained, and the kernels were visually classified as either white or red. All classifications were performed in duplicate.

2.6 FHB Kernel Determination

Only the kernels showing distinct visible symptoms of FHB damage were counted as FHB-damaged, whereas the symptom-free kernels were considered undamaged. A two-step procedure was used to determine the sorting accuracy for the FHB-damaged wheat kernels. The first step involved the visual inspection and separation of the FHB-damaged kernels from the samples sorted and classified as undamaged kernels and the separation of the undamaged kernels from the samples sorted as FHB-damaged. The second step further distinguished the FHB-damaged kernels from the portion classified as undamaged by using color images of each kernel produced by using a flatbed scanner (Expression 1680, Epson, Long Beach, CA, USA). The images were obtained with the scanner cover in the fully opened position, which resulted in a black image background. The ImageJ image-analysis software (Rasband, 2005) was used to make a final determination regarding the FHB-damaged kernels based on a preselected color threshold for the undamaged and FHB-damaged wheat kernels. All classifications were performed in duplicate. It should be noted that this method of visual classification disregards several other FHB-damaged kernels that may exhibit few or no symptoms but contain mycotoxins associated with FHB damage (Peiris et al., 2010).

2.7 Protein Content Measurement

The Perten DA7200 (Perten Instruments, Springfield, IL, USA) instrument equipped with a micromirror module sample presentation system was used to determine the protein content of the wheat kernels. The instrument was set at four repeats and two repacks, and a sufficiently sized sample (approximately 300-320 kernels) was used to completely cover the mirror and fill up the mirror module. The protein content predictions were provided based on a percent dry basis, and all measurements were taken in duplicate.

3. Results

3.1 Sorter Performance Test Results

3.1.1 Separation of red and white winter wheat

Table 1 shows the average and standard deviations of the color separations for the wheat blends (90% red and 10% white), as verified by the NaOH staining and visual separations of seed. Using two passes, the LED-based instrument removed 98% ± 0.3% of the white wheat while also removing 23.7% ± 1.7% of the red wheat. In contrast, the color image-based sorter removed fewer of the white wheat kernels (83%±1.2%) while removing more of the red wheat kernels

(42.4%±5.8%). On average, during the first pass through the sorters, the LED-based instrument removed 85.7 ± 9.6% of the white wheat while also rejecting 9.7 ± 1.9% of the red wheat. For the color image-based sorter, the first pass through the sorter removed 67.8 ± 12.4% of the white wheat while also classifying 22.9 ± 3.6% of the red wheat as white wheat. When mixed, all of these samples were difficult to visually distinguish. However, of these samples, those from the HRW variety Fuller appeared to have more weather damage and thus a lighter appearance, which made this variety visually more difficult to distinguish from the white wheat variety samples. The image sorter rejected an average of 26.2 ± 1.3% of the sample coming from Fuller and 19.7 ± 1.3% of the sample coming from Jagger. Conversely, the LED-based instrument was more consistent across the two HRW varieties, rejecting 9.7 ± 1.0% and 9.6 ± 2.6% of the samples from Fuller and Jagger, respectively. It should be noted that in previous studies the image-based sorter typically had an accuracy of 85 to 95% for most red and white samples (Pearson, 2010), and the samples used in this study were specifically chosen because they were challenging to visually distinguish.

The calibration procedure used for the LED-based sorter selected the red and green chromaticities and the ratio of the reflectance readings from the 940 nm and 1070 nm LEDs. The average 940/1070 nm ratio was higher for the red kernels than for the white, as was the red chromaticity. However, the average green chromaticity was lower for the red kernels than for the white. The differences in the chromaticity values for the red and white wheat may be due to the red wheat reflecting a higher proportion of red light, making the red chromaticity higher and the green chromaticity lower than for the white kernels. It is not known why the near-infrared reflectance ratio contributes to the successful classification of red and white wheat. Wang et al. (1999) developed neural network calibrations for distinguishing red and white wheat using visible and NIR spectra, and they reported that a portion of the absorbances near 940 nm and 1070 nm also contributed to the classifications. Another possible explanation for the sorting accuracy difference between the sorters is that the emission spectra from the red, green, and blue LEDs are more distinct and have less overlap than the transmission spectra of the color filter used on the image-based sensor.

Table 1 Average weight percent of red and white kernels rejected in the two sorting operations using the image- and LED-based sorters (standard deviations are shown in parentheses)

	Percent of original kernels rejected 1st Pass		Percent of original kernels rejected 1st + 2nd Pass	
Sorter	white	red	white	red
Image	67.8 (12.4)	22.9 (3.6)	83.0 (1.2)	42.4 (5.8)
LED	85.7 (9.6)	9.7 (1.9)	98.0 (0.3)	23.7 (1.7)

3.1.2 Separation of FHB-damaged kernels

Both the LED-based sorter and the color image sorter removed 90 ± 5.5% of the kernels with obvious visible symptoms of FHB damage.. However, the LED-based sorter removed fewer undamaged kernels (1.9%) than the color image-based sorter (7.0%). The image-based sorter rejected 17.4% of the undamaged seeds derived from Fuller HRW samples primarily because these seeds were quite light in color due to weathering. For all of the other samples, the image sorter rejected an average of 4.9 ± 2.2% of the undamaged kernels. Surprisingly, the samples with the lowest undamaged kernel rejection rate for the LED-based sorter were derived from Fuller. Similar to the red-white wheat sort, the LED calibration procedure selected certain NIR features that appear to have facilitated a more accurate sorting of the FHB-damaged and undamaged kernel mixtures. The calibration procedure for the LED sorter selected three values as the best features for the classifications; the red chromaticity and the red/850 nm and 940/850 nm ratios. Delwiche (2008) and Peiris et al. (2010) have noted several visible and NIR combinations that produce an accurate sorting of the FHB-damaged kernels. The visually FHB-damaged kernels have a higher reflectance at all three of the NIR LED wavelengths used, and the visually FHB-damaged kernels also have lower red chromaticity values than the undamaged kernels because their white appearance produces higher proportions of reflectance from the blue and green spectral bands. The higher proportion of blue and green light reflected results with a lower overall proportion of red light reflected, even though the absolute amount of red light was actually higher visually FHB-damaged kernels. Due to their white appearance, the FHB-damaged kernels reflect more visible light than the undamaged kernels, causing the ratio of red/850 nm to be higher for the visually FHB-damaged kernels than for the undamaged kernels.

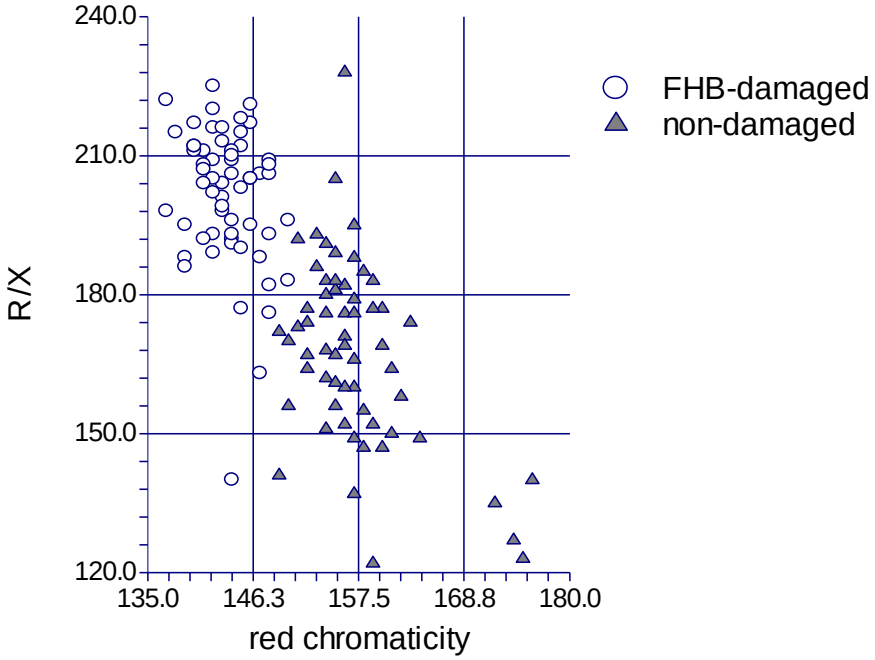

Fig 5. Ratio of *R/X* (the integrated reflectances from the red and 850 nm LEDs subtracted by the background) vs. red chromaticity as measured by the LED instrument for FHB-damaged and undamaged wheat kernels.

As demonstrated in Figure 5, only two of the three features selected, the red chromaticity and red/850 ratio, can be used to achieve satisfactory discrimination between the FHB and undamaged kernels.

3.1.3 Sorting hard red winter wheat based on protein content

The average results from the sorting of the kernels by high, intermediate, and low protein content for all seven of the hard red winter wheat varieties tested are shown in Tables 2 and 3. On average, the SKNIR, LED and color image sorters isolated the kernels with 1.9%, 1.1% and 1.0% higher protein than the original sample, respectively. These results were achieved by diverting 37.7 ± 4.8% (LED sorter) and 40.1% ± 14.9% (image sorter) of the kernels with a higher protein content from the original sample into the high protein content group using two passes through the sorter. Similarly, for the SKNIR, 40.3% of the high protein content kernels were isolated in one pass through the sorter, which resulted in a 1.9% higher protein content than that in the original sample. As may be expected, the SKNIR sorter performed better than the other two sorters in isolating higher protein content kernels, likely due to its use of a full spectrum (950-1650 nm) calibration where several absorption bands for protein are located. However, as a practical consideration, both the LED- and image-based sorters perform much faster and cost much less to build than the SKNIR. The similarity of results between the LED- and image-based sorters indicates that both instruments might preferentially select the lighter color, "yellow berry" kernels suspected as having lower protein content, and in part, this type of selection is what both sorters were calibrated to do. Additional study is needed to confirm the utility of both machines for the selection of higher protein content kernels independent of the kernel size and color. The LED sorter was more consistent than the image-based sorter in isolating higher protein content kernels across the seven different samples of hard red winter wheat because the standard deviation (in weight percent) diverted to the high protein content stream was 4.8% compared to 14.9% for the image-based sorter. As shown in Table 3, the standard deviation of the protein content change from the original sample's protein content for the LED sorter was half of that for the image sorter (0.5% vs. 1.0%). The range of protein content changes in the high protein category for the image sorter was −0.2% to 2.8%, whereas the changes from the LED sorter ranged from 0.2% to 1.7%. This result indicates that the LED sorter is less affected by the lighter-colored kernels as a result of weathering and may be better able to measure the attributes correlated with the actual protein levels. However, additional testing is needed to confirm this observation and optimize the LED emission wavelengths for better separation of the kernels by the protein content.

The calibration procedure for the LED protein sorting tests selected the reflectance of the red and 940 nm LEDs and the ratio of the 850/1070 nm LEDs. The reflectance of the red LED simply segregates the kernels using the visual lightness or darkness. On average, the reflectance at 940 nm is higher for the higher protein content kernels, whereas the ratio of 850/1070 nm is lower for the higher protein content kernels. The measured differences in the reflected light emitted by the three NIR LEDs may be due to overtones in the protein absorption bands or other physical characteristics of the kernels that are tangentially related to the protein content.

Table 2 Average protein content of the samples sorted using the SKNIR, LED, and image sorters (standard deviations are shown in parentheses)

Sorter	Protein Content by Sorting Category, %db		
	High	**Intermediate**	**Low**
SKNIR	15.8 (1.3)	13.3 (1.1)	11.8 (0.9)
LED	15.0 (0.8)	13.9 (1.2)	12.8 (1.3)
Image	14.9 (0.7)	13.7 (0.8)	12.6 (1.3)

Table 3 Average change in protein content

Sorter	Protein Content Difference from Original Sample by Sorting Category, %db		
	High	**Intermediate**	**Low**
SKNIR	1.9 (0.7)	-0.6 (0.4)	-2.1 (0.6)
LED	1.1 (0.5)	-0.1 (0.5)	-1.1 (0.4)
Image	1.0 (1.0)	-0.2 (0.6)	-1.3 (0.6)

4. Discussion

The LED instrument is promising as an accurate and low-cost instrument for sorting based on the three wheat kernel characteristics tested. However, in this feasibility study, the wheat samples tested were rather small, requiring less than 30 min each for two passes through the sorter. Additionally, the sorting of all the samples for each of the tests was performed in a single day. Additional testing is needed to determine the long-term stability of the instrument and the frequency with which recalibration should occur. However, past experience with LED illumination indicates that instruments based on this technology can be highly stable for weeks (Pearson, 2010). The original calibration samples can be saved and reused for recalibration, which can be performed in only a few minutes.

The LED-based instrument was designed with a high pulse rate because it was considered important to acquire a set of pulses from all of the LEDs before the position or orientation of the kernel changed. Faster pulse rates could be attained by the use of different microcontrollers or by switching the LEDs during the A/D conversion execution. To reduce the analog noise induced by the switching, these operations were not performed in this study according to the recommendations in the microcontroller documentation (Anonymous, 2011). Higher-resolution A/D conversions can also be acquired at the expense of slower pulse rates. More testing is needed to determine the optimal pulse rate and A/D resolution.

The six LEDs used in this study were selected because they are widely available and because they span the largest spectral range possible considering the sensor used. This configuration may be

desirable for general-purpose applications but may not be optimal for some specific applications, such as sorting for high protein content and symptomless FHB damage (Peiris et al., 2010). For example, Pasikatan and Dowell (2004) found that similar increases in the protein content (~1%) could be achieved by optical sorting when using a filter combination of 920 and 1660 nm. It was noted that the 1660 nm band was most useful for the separation of high and low protein content kernels. For the LED-based sorter, additional testing is needed in which visible and near-infrared spectra are used to select a set of LEDs that will be optimal for sorting kernels with a high protein content and symptomless FHB-damaged kernels. Selecting the optimal configuration will be the focus of future work. Additionally, InGaAs LEDs and sensors will be considered for future applications so that longer wavelengths up to 1700 nm can be included as part of the sorting process.

5. Conclusion

We confirmed the feasibility of performing rapid multispectral measurements and separating hard red wheat from hard white wheat kernels, symptomatic FHB-damaged from undamaged kernels, and kernels with different levels of protein content. The LED-based sorter performed as well as or better than a currently available color image-based sorter, although the throughput of the LED instrument was approximately 20 kernels/s compared with 200 kernels/s for the color image-based sorter. The LED-based sorter was not able to isolate the high-protein kernels as well as the InGaAs SKNIR sorter, but it performs this task at a much higher throughput and potentially at a much lower cost. Additional testing will help determine the optimal configuration of LEDs for use in different applications, and the full utility of the instrument will be determined by implementing larger-scale and longer-term tests.

Acknowledgement

The authors wish to thank Anne Berry, Biological Science Aid, for assistance in fabricating printed circuit boards in support of this project.

Disclaimer

Mention of trade names or commercial products in this publication is solely for the purpose of providing specific information and does not imply recommendation or endorsement by the U.S. Department of Agriculture. USDA is an equal opportunity provider and employer.

References

AACC International Approved Methods of Analysis, 11th edition. Method 55-31.01. Single-Kernel Characterization System for Wheat Kernel Texture. Approved November 3, 1999. AACC International, St. Paul, MN, USA.

Anonymous. 2011. ATmega48A/PA/88A/PA/168A/PA/328/P Complete Datasheet. Atmel Corporation, San Jose, CA, USA. In: http://www.atmel.com/Images/8271S.pdf , Accessed June, 2012

Delwiche, S.R. 2008. High-speed bichromatic inspection of wheat kernels for mold and color class using high-brightness pulsed LEDs. Sensing and Instrumentation for Food Quality and Safety 2:103–110.

http://dx.doi.org/10.1007/s11694-008-9037-1

Dexter, J.E., Marchylo, B.A., MacGregor, A.W., and R.Tkachuk. 1989. The structure and protein composition of vitreous, piebald and starchy durum wheat kernels. Journal of Cereal Science 10(1):19-32 http://dx.doi.org/10.1016/S0733-5210(89)80031-1

Dowell, F.E., Maghirang, E.B., Graybosch, R.A., Baenziger, P.S., Baltensperger, D.D., and L.E. Hansen. 2006. An automated near-infrared system for selecting individual kernels based on specific quality characteristics. Cereal Chemistry 83(5):537-543. http://dx.doi.org/10.1094/CC-83-0537

Dowell, F.E., Maghirang, E.B., and P.S. Baenziger. 2009. Automated single-kernel sorting to select for quality traits in wheat breeding lines. Cereal Chemistry 86(5):527-533. http://dx.doi.org/10.1094/CCHEM-86-5-0527

Hansen, P.W., Henriksen, L., Kjær, L., and J.R. Jørgensen. 2006. Multispectral imaging for detection of grain vitality. Poster presented at the 12th Australian Near Infrared Spectroscopy Group Conference, May 7-10, 2006, Rockhampton, Queensland, Australia.

Jaillais, B., Bertrand, D., Abecassis, J. 2012. Identification of the histological origin of durum wheat milling products by multispectral imaging and chemometrics. Journal of Cereal Science 55:210-217. http://dx.doi.org/10.1016/j.jcs.2011.11.011

Palais, J.C. 1988. Fiber Optic Communications, 3rd edition. Prentice Hall, Englewood Cliffs, NJ, USA.

Pasikatan, M.C. and F.E. Dowell. 2004. High-speed NIR segregation of high- and low-protein single wheat seeds. Cereal Chemistry 81(1):145-150. http://dx.doi.org/10.1094/CCHEM.2004.81.1.145

Pearson, T.C. 1999. Use of near infrared light transmission to automatically detect almonds with concealed damage. Lebensmittel-Wissenschaft und -Technologie. 32(2): 73-78.

Pearson, T.C. 2010. High-speed sorting of grains by color and surface texture. Applied Engineering in Agriculture. 26(3): 499-505.

Peiris, K., Pumphrey, M.O., Dong, Y., Maghirang, E.B., Berzonsky, W., Dowell, F.E. 2010. Near-infrared spectroscopic method for the identification of Fusarium head blight damage and prediction of deoxynivalenol in single wheat kernels. Cereal Chemistry. 87(6):511-517. http://dx.doi.org/10.1094/CCHEM-01-10-0006

Ram, M.S., Dowell, F.E., Seitz, L., and G. Lookhart. 2002. Development of standard procedures for a simple, rapid test to determine wheat color class. Cereal Chemistry 79(2):230-237. http://dx.doi.org/10.1094/CCHEM.2002.79.2.230

Rasband, W.S. 2005. Image J. U.S. National Institutes of Health, Bethesda, MD, USA.

Shahin, M.A. and S.J. Symons. 2009. Design of multispectral imaging system for detecting mildew damage on wheat kernels. Paper presented at the CSBE/SCGAB Conference, Prince Edward Island, Canada.

Sharma, G.C., A.D. Paul, and J.A. Bietz. 1983. Nitrogen Fertilization effects and anatomical. protein, and amino acid characteristics of yellow berry in triticale. Crop Science 23:699-703. http://dx.doi.org/10.2135/cropsci1983.0011183X002300040023x

Yeh, T.S. and S.S. Tseng. 2006. A low cost LED based spectrometer. Journal of the Chinese Chemical Society 53(5):1067–1072.

Wang, D., F.E. Dowell, and R.E. Lacey. 1999. Single wheat kernel color classification using neural networks. Transactions of the ASAE 42(1):233-240.